ELSEVIER

Journal of Alloys and Compounds 439 (2007) 312–320

Journal of ALLOYS AND COMPOUNDS

www.elsevier.com/locate/jallcom

# Pd and $ZnAl_2O_4$ nanoparticles prepared by microwave-solvothermal method as catalyst precursors

Mirosław Zawadzki *

*Institute of Low Temperature and Structure Research, Polish Academy of Sciences, P.O. Box 1410, Wrocław 2, Poland*

Received 11 April 2006; received in revised form 21 August 2006; accepted 23 August 2006

**Abstract**

Poly-*N*-vinyl-2-pyrrolidone (PVP) stabilized Pd nanoparticles and nanophase zinc aluminate spinel ($ZnAl_2O_4$) were prepared in different solvents by using microwave-assisted solvothermal method. The obtained materials were characterized by powder X-ray diffraction (XRD), transmission electron microscopy (TEM), textural studies (porosity and surface area) and other techniques, and used as precursors of heterogeneous metal colloid catalysts. A $Pd/ZnAl_2O_4$ system was found to be promising catalyst of light hydrocarbon combustion.

*Keywords:* Microwave-solvothermal method; Nanoparticles; $Pd/ZnAl_2O_4$ catalyst

## 1. Introduction

Metal nanoparticles have been attracting much attention for their intriguing chemical and physical properties and potential applications [1–3]. Among them, Pd nanoparticles are very interesting because of their catalytic properties. It is well known that the catalytic activity of supported metal particle catalyst is strongly dependent on the shape, size and size distribution of the particles [4,5]. Nanoparticle catalysts are highly active since most of the particle surfaces can be available to catalysis because chemical reactions take place mainly on the surface of the particles. It could be assumed that approximately 60% of the atoms exist on the particle surface when its diameter is lower than 3 nm. These surface atoms behave as the centers where the chemical reactions could be catalytically activated. It is generally considered that the optimum functioning of the catalyst takes place when at least 60% of atoms are surface atoms and only 40% volumetric atoms are contained inside the nanoparticle.

Conventional synthesis methods of small metal particles on inorganic supports have been investigated thoroughly and are well documented [6,7]. Commonly accepted preparation techniques involve ion exchange or impregnation of a support surface with metal salt solutions followed by calcinations and subsequent reduction with hydrogen. However, it is difficult to obtain well-dispersed metal nanoparticles with uniform size distributions. Therefore, considerable effort is focused on develop alternative synthesis methods based on electrochemical reduction, vapor deposition or sonochemistry. In recent years, new method has been developed for the preparation of heterogeneous metal colloid catalyst, referred to as the "precursor' concept [8–10]. This method involves the pre-preparation of nanosized metals with controlled properties followed by further deposition on the catalyst carrier material; subsequent heat treatment is then not required. An obvious advantage of the 'precursor" concept over conventional salt impregnation method is fact that structure and morphology of the nanoparticles can be tailored independently of the support. By this method fuel cell catalysts have been successfully prepared [11].

Mono- or bimetallic nanoparticles are usually prepared by the use of colloidal methods where metal salts may be reduced using various agents, in the presence of polymers, microemultions, ligands or appropriate solvents which act as a steric stabilizer by balancing the van der Waals forces that cause aggregation of the nanoparticles [12–14]. Tu and Liu [15] applied microwave techniques to the nanoscopic metal colloids synthesis, showing that PVP stabilized precious colloid metal clusters can be obtained by microwave heating with alcohol or glycol as a reductant. Recently, Komarneni [16,17] and researches from other groups

---

* Tel.: +48 71 3435021; fax: +48 71 3441029.
*E-mail address:* m.zawadzki@int.pan.wroc.pl.

0925-8388/$ – see front matter © 2006 Elsevier B.V. All rights reserved.
doi:10.1016/j.jallcom.2006.08.077

[18–21] have synthesized by microwave-solvothermal processing route various types of nanophase materials (including metal nanoparticles) having controlled physical and chemical characteristics. Particularly, nanomaterials with spinel structure were also prepared in this way [22,23].

The main advantages of microwave-solvothermal methods are: very fast kinetics, phase purity with better yield and high reproducibility. These methods seem then to be ideally suited for precise control of microstructure of nanoparticles. In addition, it is environment friendly because reactions are carried out in closed systems at rather low temperatures for a short time.

The purpose of the present work is to report the synthesis of polymer stabilized Pd nanoparticles under microwave-solvothermal (MS) conditions using (poly)ethylene glycol as solvent and reducing agent and PVP as the stabilizing matrix. Particularly, the effects of the concentration of PVP and palladium salt or the nature of the reducing agent on the morphology (shape and size) of the synthesized particles were studied. The utility of the microwave-hydrothermal processing route in the presence of urea for the synthesis of high surface area porous nanophase zinc aluminate $ZnAl_2O_4$ with spinel structure was also demonstrated. $ZnAl_2O_4$ is known as very interesting material for catalytic applications (mainly as catalyst support) because of its unique combination of desirable properties such as high thermal stability, high mechanical resistance, low temperature sinterability, better diffusion and low surface acidity [24,25]. Unfortunately, most of the commonly used preparative methods (high temperature calcination, coprecipitation, sol–gel) lead to the low surface area material, usually below 50 $m^2/g$ [26] while conventional catalyst supports require much higher area. Microwave-solvothermally formed Pd and $ZnAl_2O_4$ nanoparticles were used as precursors for the preparation of $Pd/ZnAl_2O_4$ system which catalytic properties were tested in hydrocarbon combustion.

The syntheses were performed using microwave reactor with sealed Teflon vessel giving autogenous pressure up to tens bar. The used methods are very rapid and effective for the preparation of well-controlled and uniform nanoparticles.

## 2. Experimental

### 2.1. Materials

Palladium chloride (Alfa Aesar, Germany); poly-*N*-vinyl-2-pyrrolidone—PVP K30 (Fluka, Germany): average molecular weight 40,000; zinc acetate dihydrate (POCh, Poland), aluminium isopropoxide (Aldrich, Germany); urea (POCh, Poland) were used as received. Organic solvents (ethylene glycol EG, diethylene glycol DEG, triethylene glycol TEG, *iso*-propanol, acetone) were analytical grade reagents and used without further purification.

### 2.2. Preparation of Pd colloids

The PVP stabilized Pd nanoparticles were prepared according to the following procedure: $H_2PdCl_4 \cdot nH_2O$ was first prepared by treatment $PdCl_2$ water solution with small amounts of concentrated hydrochloric acid. The appropriate amounts of PVP and pre-prepared $H_2PdCl_4 \cdot nH_2O$ were added together to (poly)ethylene glycol (50 ml) under stirring at room temperature. For each experiment 50 ml of precursor solution was poured in the reaction vessel. The microwave-solvothermal reactions were carried out under mild conditions of temperature 150 °C, pressure 10 bars and the hold time of 5 min. As the result, a dark-black homogeneous colloidal solution of Pd nanoparticles was obtained without any precipitate. Different Pd colloids were prepared by variation of the molar ratio of PVP to Pd precursor, the concentration of Pd precursor and the solvent used. As-prepared polyol dispersions of Pd nanoparticles were precipitated using anhydrous acetone, and then the nanoparticles were separated from the solution by centrifugation. The resultant precipitates were washed with anhydrous acetone to thoroughly remove the polyol residues and dried in vacuum at room temperature. The dry precipitates were re-dispersed in methanol prior to TEM characterization and use for catalyst preparation. The re-dispersed PVP colloids prepared by microwave-solvothermal processing route were very stable for at least several months.

### 2.3. Preparation of nanophase $ZnAl_2O_4$

The aluminium precursor for the microwave assisted hydrothermal preparation of nanosized zinc aluminate was aluminium hydroxide (AlOOH) produced through hydrolysis of solid aluminium isopropoxide for 20 min in excess of water heated at 70 °C with continuous stirring. The resultant slurry of AlOOH was still stirred and the proper amount of water solution of zinc acetate was added to obtain molar ratio of Zn:Al = 1:2; the concentration of the mixture was always below 10 wt%. The temperature of the mixture was maintained at 70 °C during subsequently stirring for 30 min. After cooling to room temperature, the controlled amount of urea (0.1 $mol/dcm^3$) was added with stirring. 50 ml of precursor solution was poured into a reaction vessel held in a microwave reactor. The microwave hydrothermal reactions were carried out at 150 °C, under pressure of 10 bar and for the hold time 5 min. The opalescent sol with no signs of precipitate was obtained. The former was filtered and washed with water. The nanoparticles in the sol were concentrated and separated from the solvent by centrifugation. The resulting gel was forced out in a wire from 3 to 4 mm in diameter by extrusion, air-dried overnight to remove any moisture, then calcined at 500 °C for 4 h, crushed and sieved into the 0.8–1.4 mm particles. Such obtained material was used as support for the preparation of $Pd/ZnAl_2O_4$ system.

### 2.4. Preparation of $Pd/ZnAl_2O_4$ catalyst

PVP stabilized Pd colloid which nanoparticles have an average size ∼2 nm was chosen as catalyst precursor. The catalyst was prepared by dipping the zinc aluminate support into methanol dispersions of the polymer-stabilized Pd colloid (∼1 mM metal concentration) at ambient temperature to adsorb the pre-prepared Pd nanoparticles. The mixture was filtered, and the solid was washed with methanol and dried under vacuum at room temperature. The calculated metal weight loading on support was kept at 0.5% {Pd loading $W = W_{Pd}/(W_{Pd} + W_{PVP} + W_{support}) \times 100\%$}. The metal content of the filtrate was evaluated by using atomic absorption spectrophotometer.

The $Pd/ZnAl_2O_4$ system was also prepared by conventional impregnation method for comparison purposes. The amount of $PdCl_2$ used for impregnation was adjusted to yield $ZnAl_2O_4$ containing 0.5 wt% of Pd. After drying at 80 °C in vacuum, the obtained material was finally heated at 500 °C for 4 h with the heating rate of 5 °C/min in dry air and subsequently activated in the presence of hydrogen at 500 °C for 1 h.

### 2.5. Methods

All the microwave assisted solvothermal (hydrothermal) reactions were performed in a microwave accelerated reaction system MW Reactor Model 02-02 (ERTEC, Poland). The system operates at 2.45 GHz frequency with 0–100% of full power (1000 W). The system is controlled by a temperature (300 °C max) or by pressure (100 bar max). Reaction vessel of 70 ml capacity is double walled vessel consisting of a Teflon TFM inner liner and cover surrounded by stainless steel shell.

UV–vis absorption spectral measurements were carried out with a UV–vis spectrophotometer Cary 5E having a spectral resolution of 0.01 nm between 300 and 700 nm (10 mm path length quartz cuvettes) to confirm the completeness of the reduction of the palladium colloids (by the disappearance of the absorption bands for the $PdCl_2$ precursor).

The particle size and morphology of the PVP stabilized palladium nanoparticles and nanosized $ZnAl_2O_4$ were characterized using a Philips CM20 SuperTwin electron microscope (TEM), which at 200 kV provides 0.25 nm resolution; the crystalline structure was determined by TEM and electron diffraction studies (SAED). Specimens for TEM were prepared by putting a droplet of the colloidal dispersion on a copper microscope gird covered with perforated carbon followed by evaporating off the solvent under IR lamp for 1 h. The mean particle diameter and size distribution were measured by counting at least 150 particles from the enlarged micrographs.

The as-prepared and heat treated samples were characterized for their phase purity and crystallinity by X-ray powder diffraction (XRD) using DRON-3 diffractometer (Ni-filtered Cu Kα radiation); a scan rate of 0.5° $min^{-1}$ was used to record the patterns in the $2\theta$ range 20–80°. The average crystallite size $D$ was calculated from the broadening of the X-ray line (1 1 1) and (3 1 1), respectively, for Pd and $ZnAl_2O_4$, using Schererr's equation, i.e. $D = k\lambda/(\beta \cos\theta)$ where $k$ = constant, $\lambda$ = X-ray wavelength (0.15418 nm) and $\beta$ = full width at half-maximum (FWHM) intensity of the diffraction line [27]. Elemental analysis and the impurity identification were done by using energy dispersive X-ray analysis, EDAX 9800, and atomic absorption spectrophotometry.

Thermal analysis was performed with Perkin-Elmer instruments (DTA 7, TGA 7). Thermogravimetry (TG) and differential thermal analysis (DTA) curves of the dried (unheated) samples of $ZnAl_2O_4$ were recorded over a temperature range up to 900 °C with a heating rate of 10 °C/min in the atmosphere of argon; sintered $\alpha$-$Al_2O_3$ was the thermally inert reference material used for the DTA.

The textural properties of $ZnAl_2O_4$ samples (surface area, pore size distribution and pore volume) were determined by nitrogen adsorption–desorption isotherms at liquid nitrogen temperature by using an automatic volumetric apparatus (FISONS Sorptomatic 1900). Prior to measurements samples were degassed at 300 °C for some hours and $10^{-3}$ Torr. The adsorption of nitrogen was followed until near saturation ($P/P_0 = 0.95$), then the desorption was followed until the closure of the hysteresis loop. The adsorption data were interpreted by the application of the conventional BET method for the determination of the surface area $S_{BET}$ ($m^2/g$) and by the application of the Horvath–Kavazoe method for the calculation of the micropore volume $V_\mu$ [28]. The total pore volume $V$ ($cm^3/g$) adsorbed near saturation was read from the adsorption isotherm. The pore size distribution was analyzed following the Dollimore–Heal (D–H) method [29], which was applied to the desorption branch of each isotherm. The mean pore size $R$ (nm) for each sample was read from the corresponding pore size distribution curve.

Activity of Pd catalyst supported on zinc aluminate in total oxidation of hydrocarbons was evaluated by comparison with conventionally prepared $Pd/ZnAl_2O_4$ in combustion of 0.5 vol% *iso*-butene in air mixture passed through a gradient less, circular-flow reactor with a space velocity of $10^3$ $h^{-1}$. The temperature inside the reactor was increased continuously from 50 to 300 °C at a rate of 2 °C/min. Conversion measurements were conducted by using a gas chromatograph after attaining the reaction temperature.

## 3. Results and discussion

### 3.1. Pd nanoparticles

UV–vis absorption spectrophotometry is a convenient method for evaluation the progress of metal colloid formation based on the corresponding UV–vis absorption spectra of the species present in the liquid medium. Relevant here was the disappearance of the absorption bands for the $PdCl_2$ precursor, located at approximately 320 and 425 nm. Completion of the reaction was evidenced by a simple continuous absorption spectrum in the visible range, which is typical for nanosized palladium colloids [30]. Typical UV–vis spectra of the starting solution and after microwave solvothermal reactions are presented in Fig. 1; $PdCl_2$ shows an absorption peak at 430 nm and product UV–vis spectrum shows an unstructured, continuous absorption without any peaks in the visible range what indicates that $Pd^{2+}$ was entirely reduced to $Pd^0$ independently of the solvent used.

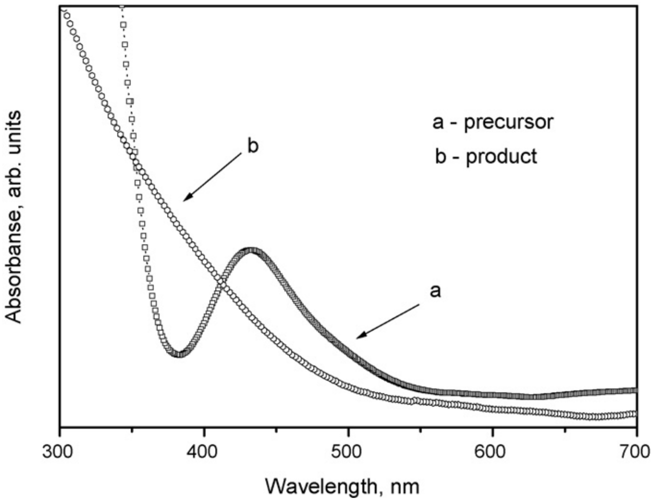

Fig. 1. Typical UV–vis absorption spectra of solution containing $H_2PdCl_4$ before (a) and after (b) microwave solvothermal processing.

The complete reduction of $PdCl_2$ to Pd metal was also confirmed by XRD analysis. The X-ray powder diffraction patterns of the samples prepared in EG solution with various PVP:Pd molar ratio are shown in Fig. 2, as an instance. As seen in this figure, several diffraction peaks are observed in the XRD patterns at $2\theta$ about 40.1°, 46.6° and 68.1°. These diffraction lines correspond to the (1 1 1), (2 0 0) and (2 2 0) reflections, respectively, for the face centered cubic (fcc) structure of Pd with space group *Fm*3*m* (according to JCPDS card no. 05-0681). The nanometer

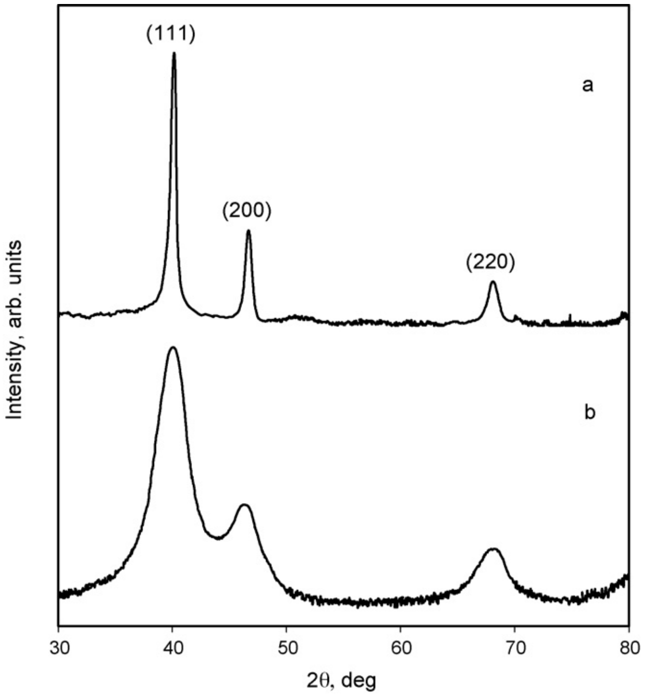

Fig. 2. XRD diffraction patterns of Pd nanoparticles prepared in ethylene glycol with PVP:Pd molar ratio of: (a) 70:3 and (b) 50:1.

Table 1
MS synthesis conditions and dimensions of PVP-stabilized Pd nanoparticles

| PVP:Pd molar ratio | Solvent (reducing agent) | Average size (nm) | Standard deviation (nm) | Relative standard deviation (nm) |
|---|---|---|---|---|
| 50:1 | Ethylene glycol | 2.0 | 0.18 | 0.090 |
| 50:1 | Diethylene glycol | 3.0 | 0.20 | 0.067 |
| 50:1 | Triethylene glycol | 3.5 | 0.28 | 0.080 |
| 50:2 | Ethylene glycol | 6.1 | 0.85 | 0.139 |
| 50:3 | Ethylene glycol | 13.0 | 1.01 | 0.078 |
| 30:3 | Ethylene glycol | 15.9 | 2.80 | 0.176 |
| 70:3 | Ethylene glycol | 11.8 | 1.12 | 0.092 |

size of the Pd crystallites is evidenced by the broad X-ray reflections. The average sizes of the nanoparticles in samples A and B were 2.3 and 11 nm, respectively, as determined from the X-ray line broadening using the Scherrer's formula.

A number of different morphology (shape and size) Pd nanoparticles were prepared by microwave-solvothermal method; synthesis conditions and dimensions of obtained particles are given in Table 1. Standard deviations were calculated from the Pd particle size distribution. It is known that relative standard deviation is a useful parameter for evaluation the dispersity of colloidal particles with different sizes. As shown in Table 1, PVP-stabilized Pd particles prepared by MS method are characterized by very good dispersity independently on the solvent used. Thus, it may be concluded that MS conditions give very uniform Pd nanoparticles in contrast to synthesis by conventional chemical reduction methods [31]. The solvents used have similar, high microwave susceptibilities which manifest themselves in the rapid temperature and pressure increase up to fixed values (150 °C, 10 bar) under solvothermal conditions. Therefore, the observed differences (not large) in the average size of Pd particles obtained by using various glycols may be affected by their diverse reducing activities at the same conditions. The size of PVP stabilized Pd nanoparticles, as can be seen from Table 1, is strongly influenced by the Pd precursor concentration or amount of PVP in reaction solution. It could be assumed, that the higher concentration of thermodynamically stable nuclei under reaction conditions leads to the smaller particle size. Because the reducing agent has to interact with the metal precursor during the reduction process, the process will be influenced by the ligands surrounding the metal ions and the reducing agent. Therefore, the size of the polymer stabilized colloidal Pd particles is governed by the interaction of the polymer with the Pd precursor and the speed of reduction. As the concentration of Pd precursor was increased, the rate of the reduction process is increased leading to an increase of the rate of crystal growth on initially formed nuclei. As the result, further nucleation is inhibited and an increase in Pd particle size could be observed. The amount of PVP added to the reaction solution may be also expected to affect the reduction of $Pd^{2+}$ as well as the growth process of Pd nanoparticles. With the decrease in the PVP to Pd molar ratio in reaction solution, the reduction of Pd ions becomes easier and the growth of the particles proceeds faster due to the lack of protecting groups, thus leading to the larger particle sizes. The smaller Pd particles, more interesting from catalytic point of view, could be formed when the higher concentration of PVP or lower content of Pd precursor is used. The effect of PVP and Pd precursor salt concentration on the mean diameter of Pd nanoparticles prepared in ethylene glycol, graphically presented in Fig. 3, clearly confirms this relationship. One can see from Fig. 3, that the average particle size increases with increasing the concentration of Pd precursor when the amount of PVP is kept constant. Meanwhile, the average particle size decreases slightly with increasing the ratio of polymer to Pd. Similar dependence was reported in the literature for polymer stabilized Pd colloids prepared by other methods [32].

Figs. 4 and 5 are typical TEM micrographs of different morphologies of microwave-solvothermally prepared Pd nanoparticles with the corresponding particle size distribution histograms. Fig. 4(a) shows a nearly uniform and high dispersion of Pd nanoparticles with average size of 2 nm, which is accompanied by very narrow particle size distribution as shown in Fig. 4(b). No shape other than spherical or quasi-spherical was observed for the nanoparticles with PVP:Pd molar ratio of 50:1. It could be noted that some of them exhibit lattice fringes of distances about 0.22 nm that well correspond to the (1 1 1) lattice plane of the fcc structure of Pd metal.

For the samples prepared with lower PVP:Pd ratios or with higher Pd precursor concentration, most of the particles have well-defined geometrical shape like these presented in Fig. 5(a), formed under PVP:Pd ratio equal 50:3. Hexagonal, triangular,

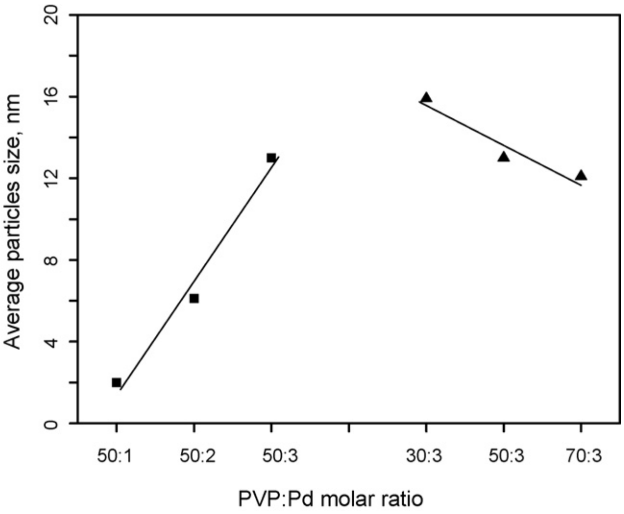

Fig. 3. Effect of stabilizing polymer (PVP) and Pd precursor salt concentration on the mean size of Pd nanoparticles prepared in ethylene glycol.

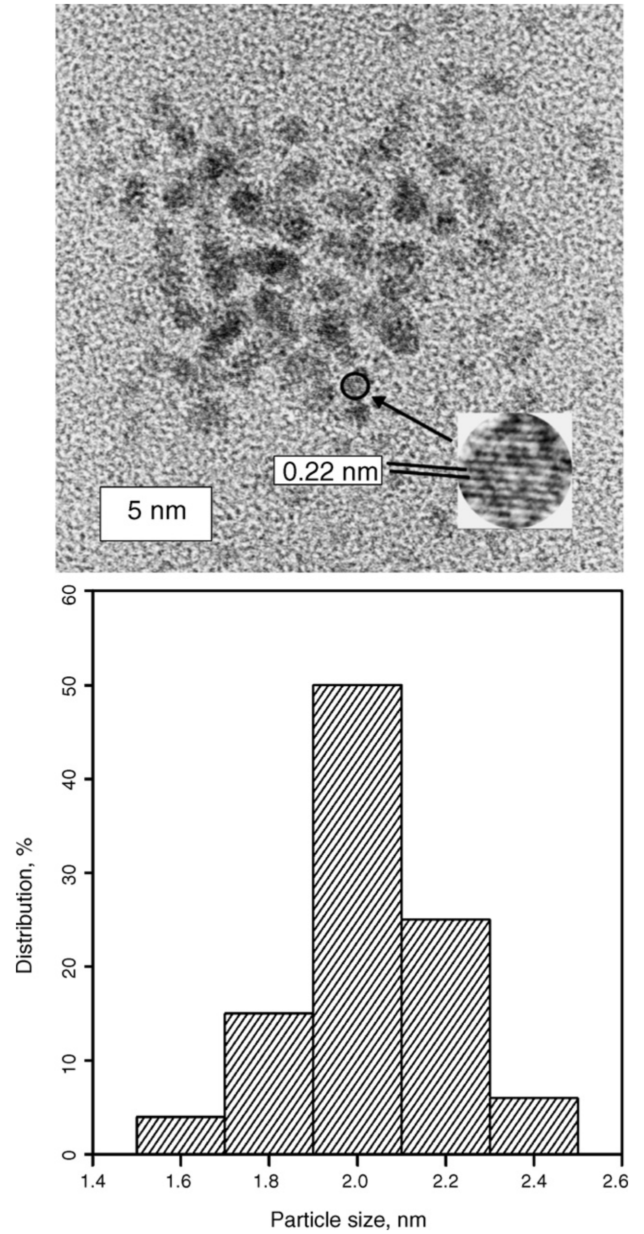

Fig. 4. (a and b) TEM image and corresponding particle size distribution histogram of PVP stabilized Pd nanoparticles prepared in ethylene glycol with PVP:Pd molar ratio equal 50:1.

rhombohedral and square are the most frequently observed particle face shapes. Similar crystal morphology has been already observed for polymer stabilized Pd nanoparticles [33]. These Pd particles are distinctly larger, have an average size of about 13 nm and are mainly distributed within the range of about 11–15 nm as shown in Fig. 5(b). The average particle sizes obtained from TEM studies were in good agreement with corresponding XRD data what suggest that individual Pd nanoparticles are nanocrystallites.

### 3.2. $ZnAl_2O_4$ material

The XRD patterns of the powder samples, as-prepared and after further heating at 500 °C are shown in Fig. 6. Extremely broad reflections are observed indicating fine particle nature of the obtained material. The observed diffraction peaks in all the recorded XRD patterns correspond to those of the standard patterns of cubic zinc aluminate spinel (JCPDS PDF No. 05-0669); no other phases were detected. These peaks can be indexed as (2 2 0), (3 1 1), (4 0 0), (3 3 1), (4 2 2), (5 1 1), (4 4 0), (6 2 0) and (5 3 3) diffraction lines. EDS analysis showed the presence of Zn and Al in the 1:2 molar ratio confirming the formation of single-phase $ZnAl_2O_4$ particles. The cubic lattice parameter was calculated from the powder XRD pattern as $a = 7.90$ and 8.01 Å for the as-prepared and heated sample, respectively, what is close to that of bulk $ZnAl_2O_4$ ($a = 8.099$ Å) as described in literature

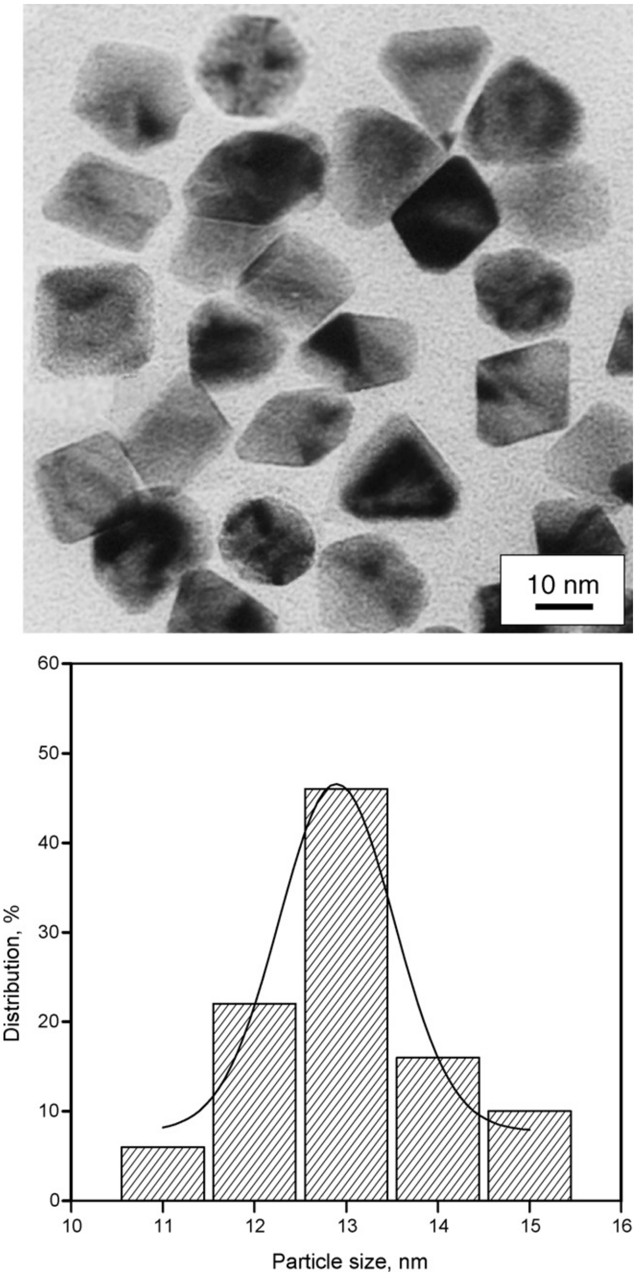

Fig. 5. (a and b) TEM image and corresponding particle size distribution histogram of PVP stabilized Pd nanoparticles prepared in ethylene glycol with PVP:Pd molar ratio equal to 50:3.

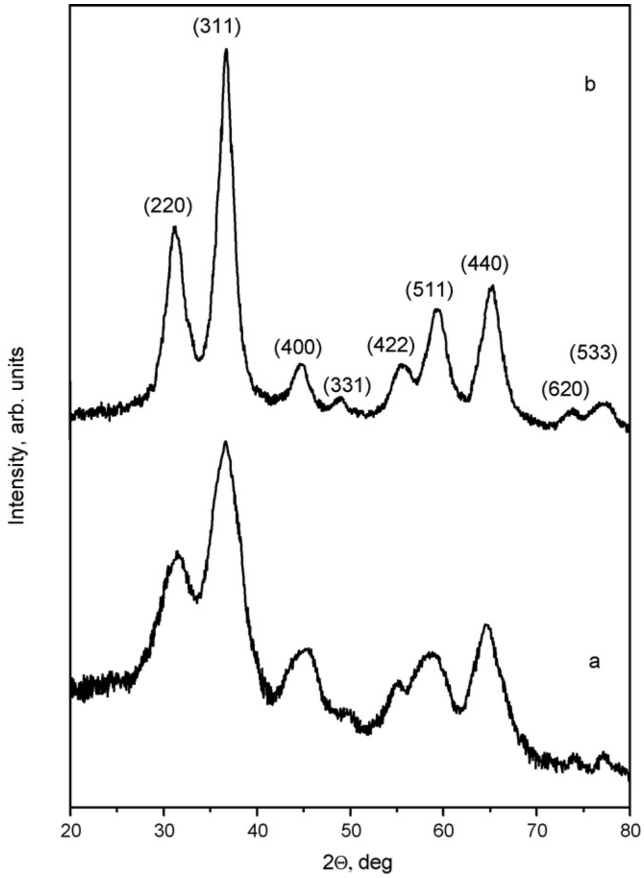

Fig. 6. XRD diffraction patterns of the as-prepared (a) and heated at 500 °C (b) $ZnAl_2O_4$ sample.

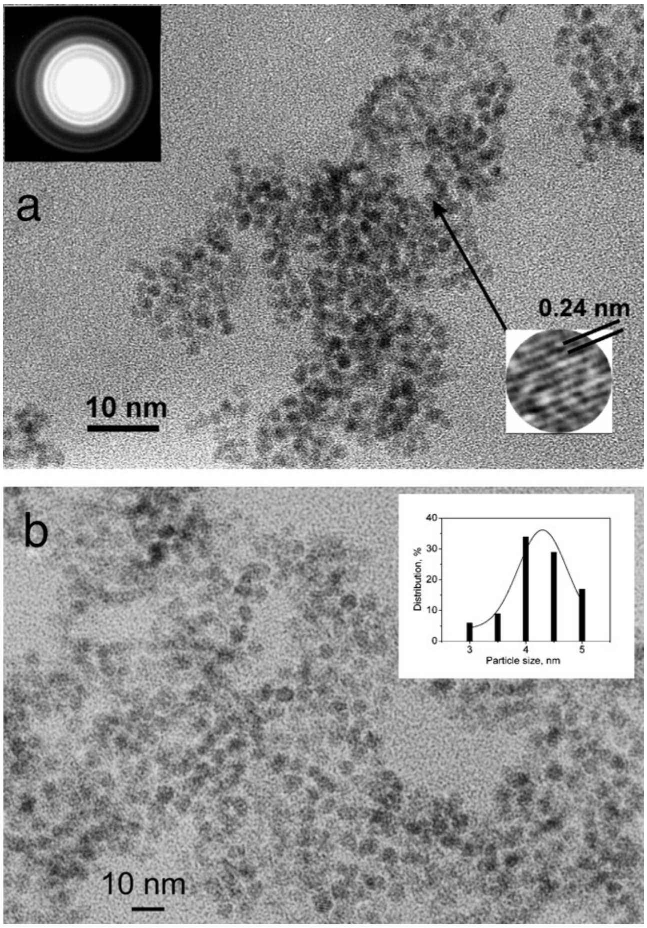

Fig. 7. TEM images of the as-prepared (a) and heated at 500 °C (b) zinc aluminate nanoparticles. The lattice fringes of distance of ∼0.24 nm on marked particle well correspond to the (3 1 1) lattice plane of $ZnAl_2O_4$. *Inset* of a exhibits the SAED pattern showing rings that match *d*-spacings for the structure of zinc aluminate spinel. *Inset* of b exhibits the particle size distribution histogram for sample heated at 500 °C.

[34]. The smaller value of the lattice parameter is probably due to the fact that the calculation of this parameter from the XRD pattern may be underestimated because of the large broadening of the reflections in the XRD pattern. It could be noticed that the diffraction peak widths decrease slightly and the intensity of the diffraction peaks increases after heating at 500 °C what is associated with an increase in the degree of crystallinity and in the crystallite size. As evident from XRD analysis, the as-prepared sample is characterized by high crystallite dispersion—the average crystallite size is ∼2.2 nm as calculated from Scherer's equation. It was found that nanocrystallinity of the microwave-hydrothermal prepared $ZnAl_2O_4$ sample was retained after heating at 500 °C; the average crystallite size increased slightly to ∼4 nm. It indicates good thermal stability of zinc aluminate obtained by this method. Similar results have been already obtained by using hydrothermal methods with conventional heating where much higher increase in the degree of crystallinity and in the crystallite size of $ZnAl_2O_4$ was observed after further heat treatment only at temperatures above 500 °C [35,36].

A representative TEM micrograph of the as-prepared sample, shown in Fig. 7(a), indicates that the nanosized particles are similarly spherical and most of them exhibit lattice fringes of distances about 0.24 nm that well correspond to the (3 1 1) lattice plane of the cubic zinc aluminate structure. Corresponding selected area electron diffraction pattern (SAED), shown in inset of Fig. 7(a), exhibits five broad rings with *d*-spacings about 0.291, 0.244, 0.203, 0.158 and 0.143 nm, which could be attributed to (2 2 0), (3 1 1), (4 0 0), (5 1 1) and (4 4 0) reflections of the cubic zinc aluminate spinel structure, respectively. The broadening of the diffraction rings suggests that the particles are small and/or are of low crystallinity. The particle size distribution obtained from TEM images is very narrow as shown in Fig. 8. The average diameter of the $ZnAl_2O_4$ particles estimated from Gaussian fit of the histogram is about 2.1 nm and is in very good agreement with that one obtained from XRD data. This consistency suggests that individual particles obtained are nanocrystallites. Also, SAED pattern of the as-prepared sample shows that the material is not fully crystalline and therefore confirms the nanocrystalline nature. TEM study of sample heated at 500 °C (Fig. 7(b)) reveals some increase in average particle size, similar to the observation of crystallite size from XRD, and some signs of agglomeration but the nanocrystalline nature of the samples is still preserved. The corresponding particle size distribution (*inset* of Fig. 7(b)) indicates the average diameter of $ZnAl_2O_4$ after heat treatment at 500 °C as 4.3 nm. It confirmed

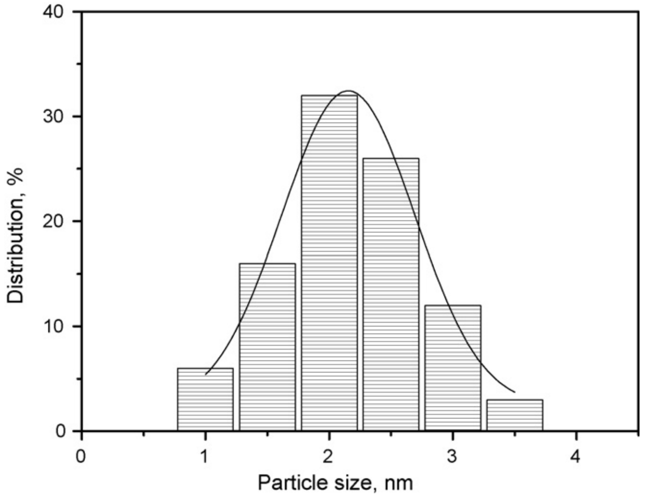

Fig. 8. Particle size distribution histogram for the as-synthesized $ZnAl_2O_4$ sample.

good thermal stability of $ZnAl_2O_4$ nanoparticles obtained under microwave-assisted hydrothermal conditions.

The typical nitrogen adsorption–desorption isotherms obtained at temperature of liquid nitrogen for the as prepared and heated sample, shown in Fig. 9, are of Type IV with H2 hysteresis loop according to IUPAC classification [37]. In the case of as-prepared sample it should be noted that adsorption takes place also at very low relative pressures what is characteristic for microporous materials. On the other hand, at the $P/P_0 > 0.1$ an increase in the adsorbed volume of nitrogen is observed due to the capillary condensation, which is characteristic for mesoporous materials. Therefore, the shape of the $N_2$ adsorption–desorption isotherms can be classified as a mixture between Types I and IV isotherms in this case. Sample heated at 500 °C shows typical Type IV adsorption–desorption isotherms with well-developed hysteresis loop. This means that this sample is mesoporous with monomodal pore size distribution and a very low contribution of micropores, responsible for the adsorption observed at low pressure. The difference between both samples can be also noticed from the moment in which the filling of all the pores with condensed nitrogen is achieved, as may be appreciated from the plateau; it starts beyond $P/P_0$ ~0.7 and 0.8, respectively, for the as-prepared and heated sample and is higher for the second one. This means that the pores in the as-prepared sample are smaller, as demonstrated by the desorption hystresis loop which is shifted to a lower relative pressure ratio. The shape of the hysteresis loops suggests that heat treatment gives rise to a broad pore size distribution in mesoporous region. Moreover, such a shape of hysteresis loop, as was observed for the heated sample, is generally characteristic for solids consisting of particles crossed by nearly cylindrical channels or made by aggregates (consolidated) or agglomerates (unconsolidated) of spheroidal particles [38].

The pore size distributions were calculated from the corresponding desorption isotherms according to the D–H method and were shown in *Inset* of Fig. 9. It indicates that pore size distributions are monomodal for both samples. In the case of the as-prepared sample a lot of pores are in the microporous region and pore size distribution has very sharp curve centered at ~1.1 nm while a little broad pore size distribution was observed for heated sample. It should be noticed that the mean pore size *R* is only slightly shifted in mesoporous region to ~2.8 nm.

The as-prepared sample is characterized by high specific surface area $S_{BET} = 210\,m^2/g$, which decreases to $160\,m^2/g$ for sample heated at 500 °C. The total pore volume *V* was similar for both samples (~$0.150\,cm^3/g$ at $P/P_0 = 0.95$) but the as-prepared sample had significant contribution of micropore volume ($V_\mu = 0.115\,cm^3/g$).

Fig. 10 shows a representative DTA and TGA curves of $ZnAl_2O_4$ sample prepared by microwave assisted hydrothermal method. The DTA analysis reveals only one significant thermal effect—sharp endothermic peak at around 132 °C, which is associated with the departure of physically adsorbed molecular water. The TGA analysis proves that this thermal effect is accompanied by weight loss. Additionally, broad and weak endothermic peak with its maximum at ~295 °C may be observed in the DTA curve as the result of the removal of zinc aluminate constitutional water. The lack of any noticeable exothermic effects

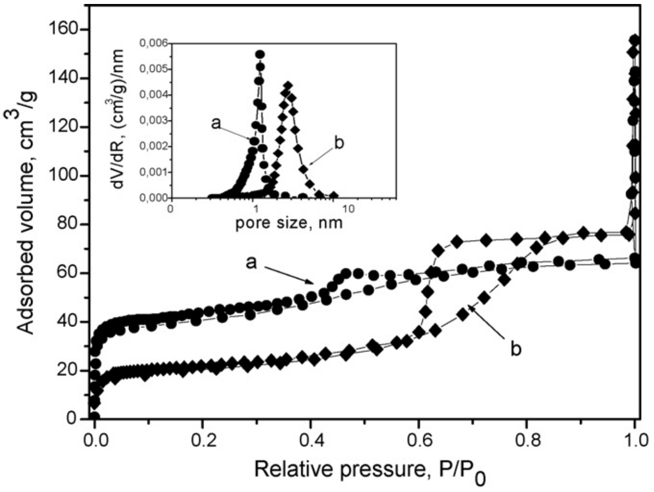

Fig. 9. Nitrogen adsorption–desorption isotherms and corresponding pore size distributions of $ZnAl_2O_4$ sample: (a) as-prepared and (b) heated at 500 °C.

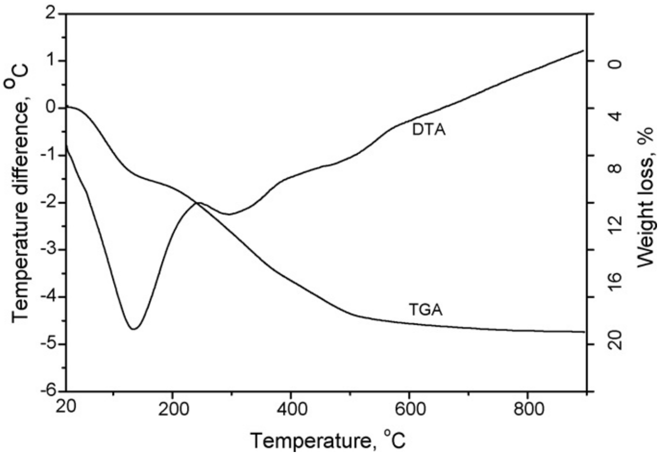

Fig. 10. DTA–TG curves of $ZnAl_2O_4$ sample prepared under microwave hydrothermal conditions.

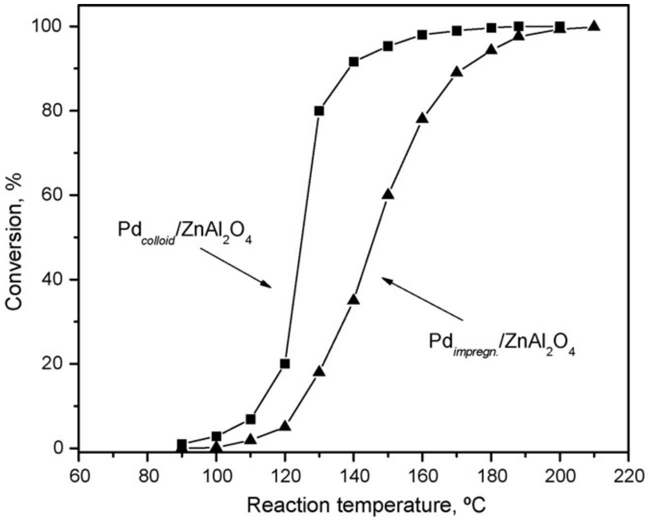

Fig. 11. Combustion of *iso*-butene over 0.5 wt% $Pd/ZnAl_2O_4$ systems obtained from pre-prepared Pd nanoparticles and by impregnation method.

suggests that no recrystallization of the dispersed $ZnAl_2O_4$ spinel occurs at temperature up to 900 °C.

### 3.3. *$Pd/ZnAl_2O_4$ system*

The catalytic activity of PVP stabilized palladium colloid supported on porous high surface area zinc aluminate, both prepared by using microwave solvothermal processing route, was evaluated in total oxidation of *iso*-butane in comparison with $Pd/ZnAl_2O_4$ system obtained by conventional impregnation method. The catalytic activities of both systems were investigated at a temperature of 50–250 °C and compared in terms of their light-off temperatures corresponding to 50% conversion. Fig. 11 presents typical *iso*-butene conversion curves as a function of increasing reaction temperature (2 °C/min). Conversion started at 90 °C and 110 °C, respectively, for the “colloid” and “impregnated” catalyst, and increased more or less rapidly with the increasing reaction temperature. Conversions of 100% could be obtained above 170 and 210 °C, respectively. It should be stated that both catalyst showed relatively high activity but reaction temperature over “colloid” catalyst was always lower by at least 20 °C for 50% conversion than over conventionally prepared catalyst. This indicates that $ZnAl_2O_4$ obtained by microwave hydrothermal method is promising catalyst support material in both cases. However, probably due to the high surface area of support as well as the high dispersion of polymer stabilized nanoparticles, the temperatures of 50 and 100% conversion were noticeable lower for the catalyst prepared from colloid nanoparticles. It is well known that the surface of the support on the molecular scale, and therefore that surrounding the active metal sites, is not well defined so it is usually difficult to obtain, by conventional impregnation method, monodispersed metals because the interaction of the individual metal atoms is high compared with the interaction between the reduced metal and the support. Additionally, active sites formed by conventional methods can be significantly contaminated with the support.

## 4. Conclusions

The proposed microwave-assisted solvothermal method is very rapid and effective for the preparation of polymer stabilized Pd nanoparticles with controllable sizes from 1.6 to 15 nm as well as single-phase zinc aluminate of particles with an average size ∼2.1 nm and narrow size distribution as were confirmed by powder X-ray diffraction and electron microscopy studies. The morphology (shape and particle size) of Pd nanoparticles is greatly affected by the concentration of the stabilizing polymer and Pd precursor salt. The nature of reducing agents (EG, DEG and TEG) used was of less significance under microwave solvothermal conditions of fixed parameters (temperature, pressure and time). Liquid nitrogen adsorption–desorption measurements revealed that nanocrystalline $ZnAl_2O_4$ exhibits interesting textural properties like high specific surface area (up to 210 $m^2/g$) and microporous structure with an average pore size about 1.1 nm. After heat treatment at 500 °C, some increase in the degree of crystallinity and a shift of pore size distribution towards mesoporous region was observed. Such properties make it a promising material for use in the development of catalyst carriers. Pd colloid nanoparticles supported on zinc aluminate spinel was found to be more active in *iso*-butane combustion than corresponding system prepared by conventional impregnation method. This indicates that nanostructured Pd colloid and porous $ZnAl_2O_4$ prepared under microwave assisted solvothermal conditions are very promising catalyst precursors.

## References

[1] G. Schmid, Clusters and Colloids, VCH, Weinheim, 1994.
[2] S. Sugano, Microcluster Physics, Springer–Verlag, Berlin, 1991.
[3] W. Yu, H. Liu, X. An, J. Mol. Catal. A: Chem. 129 (1998) L9.
[4] T.S. Armadi, Z.L. Wang, T.C. Green, A. Henglein, M.A. El-Sayed, Science 272 (1996) 272.
[5] L.G. Pratibha, R. Roper, M.G. White, Curr. Opin. Solid State Mater. Sci. 6 (2002) 401.
[6] R.D. Gonzales, H. Miura, Catal. Rev. Sci. Eng. 36 (1) (1994) 145.
[7] G. Ertl, H. Knözinger, J. Weitkamp (Eds.), Handbook of Heterogeneous Catalysis, VCH, Weinheim, 1997.
[8] H. Bönnemann, G. Braun, W. Brijoux, R. Brinkmann, A. Schulze Tilling, K. Seevogel, K. Siepen, J. Org. Chem. 520 (1–2) (1996) 143.
[9] W.R. Moser (Ed.), Advanced Catalyst and Nanostructured Materials, Academic Press, San Diego, 1996.
[10] A. Miyazaki, I. Balint, K. Aika, Y. Nakano, J. Catal. 204 (2001) 364.
[11] H. Bönnemann, K.S. Nagabhushana, J. New Mater. Electrochem. Syst. 7 (2) (2004) 93.
[12] T. Teranishi, H. Hori, M. Miyake, J. Phys. Chem. B 101 (1997) 5774.
[13] S. Chen, K. Huang, J.A. Stearns, Chem. Mater. 12 (2000) 540.
[14] X. Yan, H. Liu, K.Y. Liew, J. Mater. Chem. 11 (2001) 3387.
[15] W. Tu, H. Liu, J. Mater. Chem. 10 (2000) 2207.
[16] S. Komarneni, Curr. Sci. 85 (12) (2003) 1730.
[17] F. Gao, Q.Y. Lu, S. Komarneni, Chem. Mater. 17 (4) (2005) 856.
[18] A.V. Murugan, B.B. Kale, A.V. Kulkarni, L.B. Kunde, V. Saaminathan, J. Mater. Sci. Mater. Electron. 16 (2) (2005) 295.
[19] C.R. Patra, G. Alexandra, S. Patra, D.S. Jacob, A. Gedanken, A. Landau, Y. Gofer, New J. Chem. 29 (5) (2005) 733.
[20] A. Largeteau, S. Oree, C. Marzat, G. Demazeau, High Pressure Res. 20 (1–6) (2001) 281.
[21] Y.B. Khollam, S.B. Deshpande, P.K. Khanna, P.A. Joy, H.S. Potdar, Mater. Lett. 58 (2004) 2521.

[22] S. Verma, P.A. Joy, Y.B. Khollam, H.S. Potdar, S.B. Deshpande, Mater. Lett. 58 (2004) 1092.
[23] F. Bensebaa, F. Zavaliche, P. L'Ecuyer, R.W. Cochrane, T. Veres, J. Colloid Interface Sci. 277 (2004) 104.
[24] R. Roesky, J. Weiguny, H. Bestgen, U. Dingerdissen, Appl. Catal. A: Gen. 176 (1999) 213.
[25] H. Grabowska, W. Miśta, J. Trawczyński, J. Wrzyszcz, M. Zawadzki, Appl. Catal. A: Gen. 200 (2001) 1561.
[26] M.A. Valenzuela, J.P. Jacobs, P. Bosch, S. Reijne, B. Zapata, H.H. Brongersma, Appl. Catal. A: Gen. 148 (1997) 315.
[27] B.D. Cullity, Elements of X-ray Diffraction, second ed., Addison-Wesley, Reading, 1978.
[28] S.J. Gregg, K.S.W. Sing, Adsorption, Surface Area and Porosity, Academic Press, London, 1982.
[29] D. Dollimore, G.R. Heal, J. Appl. Chem. 14 (1964) 109.
[30] J.A. Creighton, D.G. Eadon, J. Chem. Soc. Faraday Trans. 87 (1991) 3881.
[31] Y.T. Vu, J.E. Mark, Colloid Polym. Sci. 282 (2004) 613.
[32] H.P. Choo, K.Y. Liew, H. Liu, J. Mater. Chem. 12 (2002) 934.
[33] H.P. Choo, K.Y. Liew, W.A. Mahmood, H. Liu, J. Mater. Chem. 11 (2001) 2906.
[34] H.Z. Saalfeld, Z. Kristallogr. 120 (1964) 476.
[35] J. Wrzyszcz, M. Zawadzki, A.M. Trzeciak, J.J. Ziolkowski, J. Mol. Catal. A: Chem. 189 (2002) 203.
[36] M. Zawadzki, J. Wrzyszcz, Mater. Res. Bull. 35 (2000) 109.
[37] IUPAC Recommendations, Pure Appl. Chem. 66 (1994) 1739.
[38] J. Roquerol, et al. (Eds.), Characterization of Porous Solids III, Elsevier, Amsterdam, 1994.